Available online at www.sciencedirect.com
SCIENCE DIRECT®
Biochemical and Biophysical Research Communications 325 (2004) 203–214
BBRC
www.elsevier.com/locate/ybbrc

Cellular signaling mediated by calphoglin-induced activation of IPP and PGM☆,☆☆

Koichi Takahashi, Madoka Inuzuka, Tatsuya Ingi*

Department of Neurophysiology, Brain Research Institute, Niigata University, 1 Asahi-machi, Niigata 951-8585, Japan

Received 17 September 2004

Abstract

Universal protein networks conserved from bacteria to animals dictate the core functions of cells. Inorganic pyrophosphatase (IPP) is an essential enzyme that plays a pivotal role in a broad spectrum of cellular biosynthetic reactions such as amino acid, nucleotide, polysaccharide, and fatty acid biosynthesis. However, the in vivo cellular regulation mechanisms of IPP and another key metabolic enzyme, phosphoglucomutase (PGM), remain unknown. This study aimed to examine the universal protein regulatory network by utilizing genome sequences, yeast proteomic data, and phosphoryl-transfer experiments. Here we report a novel human protein, henceforth referred to as calphoglin, which interacts with IPP and activates it. Calphoglin enhances PGM activity through the activated IPP and more directly on its own. Protein structure and assembly, catalytic function, and ubiquitous cellular localization of the calphoglin (-IPP–PGM) complex were conserved among *Escherichia coli*, yeast, and mammals. In the rat brain, calphoglin mRNA was enriched in the hippocampus and the cerebellum. Further, the linkage of the calphoglin complex to calcium signaling was demonstrated by its interactive co-localization within the calmodulin/calcineurin signaling complex, by Ca^{2+}-binding and Ca^{2+}-controlled activity of calphoglin–IPP, and by calphoglin-induced enhancement of microsomal Ca^{2+} uptake. Collectively, these results suggest that the calphoglin complex is a common mechanism utilized in mediating bacterial cell metabolism and Ca^{2+}/calmodulin/calcineurin-dependent mammalian cell activation. This is the first report of an activator of IPP and PGM, a function novel to proteins.

Keywords: Calphoglin; Calcineurin; Phosphoglucomutase; Inorganic pyrophosphatase

The genome sequences of humans as well as a set of additional broad organisms represent the basic foundation of information on cellular proteins and their long evolutionary history. The most elementary cellular functions; basic metabolism, DNA replication, DNA transcription into RNA, RNA translation into protein, and the like, evolved only once and have stayed pretty well fixed since the evolution of single-celled yeasts and bacteria. Glucose metabolism and related orthologous genes are observed in every living cell, and the importance of glucose as a central signaling molecule in all cells has recently been recognized [1].

An unexpected finding that emerged from large-scale genome analyses was that prokaryotes expressed numerous genes belonging to molecular families long studied in the immune system and the nervous system of mammals. Cyclophilins, receptors for a major immunosuppressant drug, cyclosporin A (CsA), are ubiquitous proteins present in a wide variety of organisms and are abundant in mammalian lymphocytes and neurons. A CsA–cyclophilin complex acts by binding to the Ca^{2+}/calmodulin-dependent phosphatase calcineurin,

☆ A GenBank accession number for calphoglin cDNA is AY563137.
☆☆ *Abbreviations:* CsA, cyclosporin A; *E. coli*, *Escherichia coli*; IPP, inorganic pyrophosphatase; PGM, phosphoglucomutase; PPi, pyrophosphate.

* Corresponding author. Fax: +81 25 227 0814.
E-mail address: tingi@bri.niigata-u.ac.jp (T. Ingi).

0006-291X/$ - see front matter © 2004 Elsevier Inc. All rights reserved.
doi:10.1016/j.bbrc.2004.10.021

inhibiting its phosphatase activity that leads to immunosuppressant effects in T lymphocyte proliferation [2]. In the brain, a glutamate receptor-mediated influx of Ca^{2+} leads to calcineurin activation and underpins specialized higher order functions such as transcriptional neuron response. Cyclophilins and other immunosuppressant-binding proteins share one commonality, peptidylprolyl isomerase activity [3]. Prokaryotes have peptidylprolyl isomerase proteins that exhibit extensive sequence homology to mammalian cyclophilins. Still, the link between cyclophilin/calcineurin signaling and cellular metabolic activation mechanism remains unclear.

One of the primary goals of postgenomic biology is to understand how distant orthologues result in the concerted action of gene products to generate a common function, "cellular activity." Recent analyses of yeast protein complexes on a proteome-wide scale have resulted in significant progress being made towards this goal [4–6]. Such studies have identified hundreds of distinct multiprotein complexes in the budding yeast *Saccharomyces cerevisiae* using two-hybrid methods and affinity purification. The data provide an outline of an organism's proteome as a network of protein complexes. Phosphoryl-transfer is the predominant strategy for the control of elaborate protein network activities in cells, and is often used as an experimental tool to identify signaling pathways in protein complexes. In eukaryotes, a series of chemically stable phosphorylations occurs in which the phosphates are transferred from ATP molecules to tyrosine, serine, and threonine residues of proteins by the respective protein kinase. In contrast, the transfer of the phosphoryl group from a histidine kinase to a response regulator forms the basis of bacterial and lower eukaryotic signal transduction [7]. Phosphohistidine is chemically unstable and is often indicated by acid-unstable phosphorylation [8]. Recent examinations of archaeal, bacterial, and eukaryotic genomes, however, have revealed the widespread presence of networks of phosphoryl-transfer enzymes in all domains of life [9]. The phosphoryl-transfer enzymes include various types of kinases, ATPases, pyrophosphatases, and glycolytic phosphotransfer enzymes. These findings indicate that phosphoryl-transfer enzymes may dominate universal cellular signaling pathways in the same manner among diverse species.

In the present study, we found that calphoglin was an extremely bioactive molecule in *Escherichia coli* cells. Calphoglin enhanced IPP activity which sequentially activated PGM in prokaryotic and eukaryotic cells, consistent with their postulated role as universal cellular signaling pathways. The functional protein complex of calphoglin, IPP, and PGM is henceforth referred to as the calphoglin complex. The calphoglin complex is a crucial apparatus involved in linking the principal cellular metabolism (phosphate and glucose metabolism) with other core functions of cells (protein synthesis and degradation, calcium signaling, and cell growth).

Materials and methods

Protein expression, E. coli lysates, and phosphorylation experiment. The cDNAs of human calphoglin and *E. coli* PGM were subcloned into the *E. coli* expression vectors of pDEST14, pDEST17, and pET-DEST42 (Invitrogen). The cDNAs of *E. coli* IPP and human PGM1 in pCA24N vectors (AB052891) were also used. The *E. coli* strains, BL21-AI and BL21-SI (Invitrogen), were transformed with these plasmids, and 5 ml of cultures was induced by 0.2% arabinose and 0.3 M NaCl, respectively, to express proteins. The cells were harvested 2 h after the induction by centrifugation and 0.3 ml of the resuspended cells was sonicated on ice using a microprobe for 1 min. Each 25 μl of phosphorylation reaction mixture contained 50 mM Tris–HCl, pH 7.5, 10 mM $MgCl_2$, 20 μCi [^{32}P]ATP, and 30 μg lysate protein. After 60 min of incubation at 25 °C, the reactions were stopped by a 5 μl of 6× SDS loading buffer. For the autophosphorylation of purified PGMs, a 25 μl reaction mixture contained 50 mM Tris–HCl, pH 7.5, 5 mM $MgCl_2$, 1 mM dithiothreitol, 1 mM EDTA, 50 μM [^{32}P]ATP (50 μCi), and 5 μg PGM.

Protein purification, Western blot, and antibody production. After the induction of 400 ml cultures, the cell suspension was sonicated on ice using a microprobe for 40 min. The cell lysate was centrifuged at 12,000*g* for 15 min at 4 °C. From the supernatant, expressed $(His)_6$-tagged proteins were affinity-purified using an immobilized Ni^{2+}-column (Amersham, Product Number 17-1880-01) and a PD-10 desalting column (Amersham) as described in the manufacturer's protocols. Western blot analysis using anti-V5 antibody (Invitrogen) was performed at a 1:7000 dilution as described in the manufacturer's protocol. Anti-calphoglin rabbit polyclonal antiserum was generated against a full-length recombinant protein and used at a 1:4000 dilution.

PGM assay and rat soluble protein fraction. A 1 ml reaction mixture contained 20 mM Tris–HCl, pH 7.5, 10 mM $MgCl_2$, 1 mM glucose-1-phosphate, 0.25 mM $NADP^+$, and 0.1 mM glucose-1,6-diphosphate. The reaction was initiated by addition of the indicated amount of cell lysates or purified PGM proteins, and 1 unit of glucose-6-phosphate dehydrogenase. The reduction of $NADP^+$ was measured every 30 s for 20 min at 25 °C with a spectrophotometer (340 nm). To prepare soluble protein fractions, 5 g of rat skeletal muscle was minced and cooled in 50 ml of 25 mM Tris–HCl, pH 7.4, 137 mM NaCl, and 2.7 mM KCl. The minced muscle was then homogenized for 15 min. The homogenate was centrifuged at 5000*g* for 10 min at 4 °C. The supernatant was then centrifuged at 12,000*g* for 10 min and the resulting supernatant was collected for PGM and IPP assays.

IPP assay and total cellular Pi. The reaction mixture contained 20 mM Tris–HCl, pH 8.0, 10 mM $MgSO_4$, 60 mM KCl, 2 mM PPi, and the indicated amount of IPP or cell lysates in a total volume of 0.1 ml. The reaction was initiated by adding 4 μl of 50 mM PPi. After incubation at 30 °C for 30 min, the reaction was terminated by adding 4 μl of 1 M citric acid. To determine the rate of PPi hydrolysis, the release of Pi was measured by the colorimetric method as previously described [10]. In experiments of calphoglin-dependent IPP enhancement, 30 ng of each purified IPP protein of yeast and *E. coli* (Sigma) or 55 μg of rat muscle protein was incubated with 300 ng of affinity-purified calphoglin protein for 10 min at 25 °C, and IPP activity was assayed for 30 min. In experiments of Ca^{2+}-dependent IPP inhibition, the reaction mixture contained 2 mM $MgSO_4$. Total cellular Pi was extracted from 60 mg dry pellets of *E. coli* cultures with 1.2 ml of 1 M HCl.

RT-PCR. RT-PCR of calphoglin mRNA used the primers 5′-cttggggaggagttggccagtgcagcag-3′ and 5′-atcaggactgacttctcatcttcagcctcc-3′. RT-PCR of PGM used the primers 5′-ggtgttctgggaaagcagcagtttgact

tggaaaa-3′ and 5′-tcgtttgctgagaactgcttccccacaaaggagcg-3′. The both amplifications were performed under the following conditions: denaturation at 94 °C for 1 min, denaturation at 94 °C for 45 s, annealing at 68 °C for 1 min, primer extension at 72 °C for 1 min for 30 cycles, and final primer extension at 72 °C for 5 min.

In situ hybridization. Experiments were performed as previously described [11] using ^{35}S-labeled riboprobes of full-length calphoglin.

Two-hybrid experiments. Experiments were performed as previously described [12] with some modifications indicated in figure legend. Transformation of pOBD2-vector into each ORF transformant was performed using S.c.EasyComp transformation kit (Invitrogen). The yeast suspensions were plated onto synthetic plates lacking tryptophan and leucine, and were incubated for 7 days at 30 °C. After colonies had grown they were picked and plated onto synthetic plates lacking tryptophan, leucine, and histidine to detect two-hybrid activation. Control transformations were included in each assay, without insert and with only pOBD2-*calphoglin* (or -*E. coli pgm*).

Cell culture. SV-40 transformed African Green Monkey Kidney (COS-7) cells (Japan Health Sciences Foundation) were cultured in DMEM supplemented with 10% fetal bovine serum. Approximately 1×10^5 cells in a well were transfected with the lipoplexes containing 5 μg of each DNA of pcDNA/DEST47-calphoglin, pcDNA3.2/V5DEST-calphoglin, and their empty vectors (Invitrogen).

$^{45}Ca^{2+}$-binding experiments. Experiments were performed as previously described [13]. Proteins were separated by SDS–PAGE on 12% gels and transferred onto a nitrocellulose membrane. After transfer, the membrane was incubated with 1 μCi/ml $^{45}Ca^{2+}$ for 10 min at 25 °C in a solution containing 10 mM imidazole–HCl, pH 6.8, 60 mM KCl, and 5 mM $MgCl_2$. The membrane was rinsed with distilled water for 5 min, then air-dried, and exposed to X-OMAT film for 1–5 days.

$^{45}Ca^{2+}$ uptake experiments. Microsomal fractions were prepared from rat muscle tissue as previously described [14]. Twenty-five microgram microsome, 3μg calphoglin, and 0.3 μg yeast IPP were incubated at 37 °C in 1 ml of 20 mM Mops, pH 7.2, 100 mM KCl, 20 mM NaCl, 5 mM $MgCl_2$, 3 mM ATP, 5 mM NaN_3, 2 mM PPi, 20 μM $CaCl_2$, and 1.2 μCi $^{45}CaCl_2$. After the indicated time, $^{45}Ca^{2+}$ accumulated by microsomes was measured by the rapid-filtration technique previously described [15].

Results and discussion

Calphoglin induces the phosphorylation of E. coli PGM and increases its activity

To capture common components associated with phosphoryl-transfer signaling in prokaryotic and mammalian cells, mammalian cDNA-expressing *E. coli* cells were screened using an in vitro [^{32}P]ATP labeling method. Using a BLASTP search, we ascertained 50 unknown mammalian gene products having homology to bacterial and fungal phosphoryl-transfer enzymes such as histidine kinases. The mammalian cDNAs were transfected to an *E. coli* strain, BL21-AI, the ensuant colony cultures were induced by 0.2% arabinose to express the proteins, and the cell lysates phosphorylated with [^{32}P]ATP.

The expression of a human brain cDNA clone (calphoglin, calcium–phosphate–glucose-linkage) exhibited the significant increase in the phosphorylation of the 55 kDa protein (Fig. 1A) and suppressed host *E. coli* cell growth (Fig. 1C), while the expression of other clones had no effect on the protein phosphorylations or phenotypes. Similarly, the expression of C-terminal $(His)_6$-V5-tagged calphoglin specifically increased the phosphorylation of a 55 kDa protein. In contrast to the acid-unstable nature of most prokaryotic phosphoproteins [8], the phosphorylation of the 55 kDa protein was acid-stable, which is characteristic of eukaryotic proteins. The expressed recombinant calphoglin was purified by a Ni^{2+}-column, visualized by Coomassie (CBB) stainings, and recognized specifically by anti-V5 antibodies (Fig. 1B). A full-length calphoglin protein migrates as a major band at 80 kDa, and a secondary 35 kDa band represents C-terminal cleavage products. Calphoglin mRNA is 2.9 kb long and encodes a protein of 691 amino acids (Fig. 2A), which is consistent with the size of the expressed recombinant protein. We purified the 35 kDa fragment using a Ni^{2+}-column and two-dimensional PAGE, and analyzed the N-terminal amino acid sequence. The obtained sequence corresponded to the (497–503) amino acids of calphoglin protein, which identifies the cleavage site as being between the 496th and the 497th amino acid residues of calphoglin (Fig. 2A). The results from utilizing another tightly regulated expression system using 0.3 M NaCl as an inducer (Fig. 1A, right panel) confirmed the calphoglin protein, not the inducers, was responsible for the increase in phosphorylation.

To identify the 55 kDa phosphoprotein, we purified the protein using combinatorial chromatography and two-dimensional PAGE, and analyzed the N-terminal amino acid sequence. The sequence obtained for the 55 kDa protein was AIHNRAGQPAQQ, which corresponds to the N-terminal (2–13) amino acids of *E. coli* PGM protein [16]. PGM catalyzes the interconversion of glucose-1-phosphate and glucose-6-phosphate, and is a critical enzyme in both glucolysis and gluconeogenesis. In this enzyme mechanism, a phosphoryl group is transferred from the active phosphoenzyme to glucose-1-phosphate, forming a dephosphoenzyme-glucose-1,6-diphosphate intermediate, which then rephosphorylates the enzyme to yield glucose-6-phosphate. The presence of the phosphorylated enzyme of PGM has been found in all cellular organisms (archaea, bacteria, and eukaryote) with highly conserved structures [16,17]. To examine the relationship between PGM phosphorylation and its activity, we measured the enzyme activity of PGM in lysates of calphoglin cDNA- and vector-transfected *E. coli* cells. The reaction velocity of the phosphorylated PGM was 1.9 ± 0.1 μmol/min/mg of protein and was found to be five times higher than that of the unstimulated protein (Fig. 1D), which agrees with a report identifying phosphorylated PGM as a catalytic active form [18]. However, the increased ^{32}P-labeling of PGM does not clearly indicate the amount of the phosphorylation level increase; rather it may reflect a

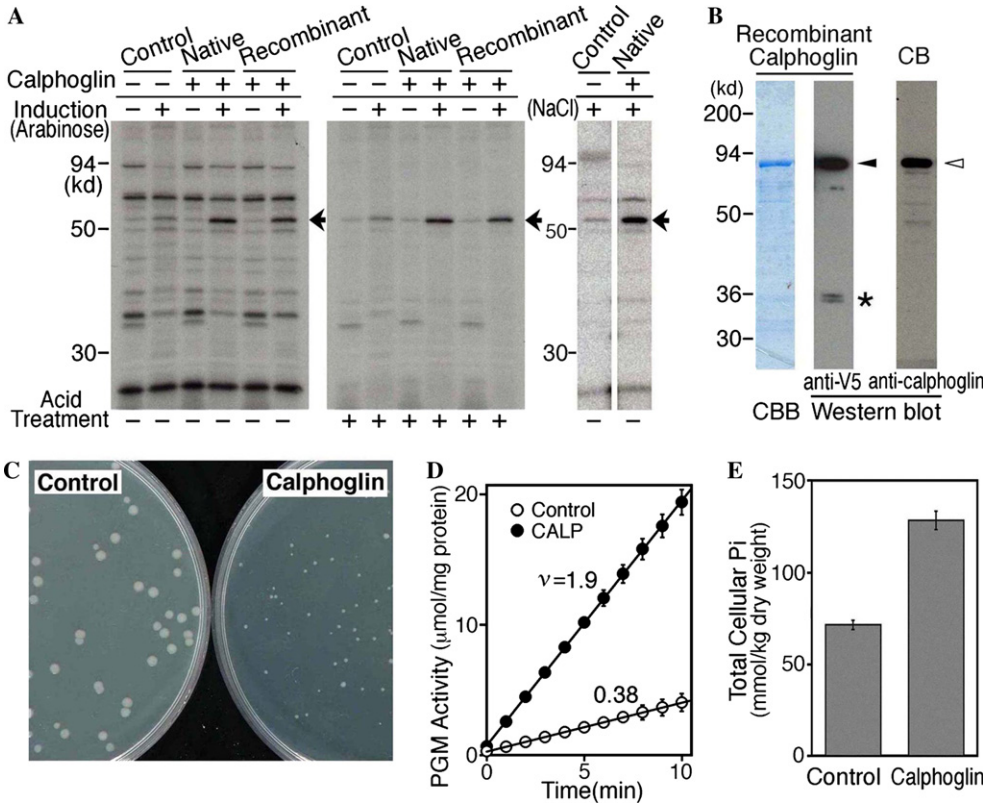

Fig. 1. Specific action identification of human calphoglin on *E. coli* cells. (A) The specific increase of acid-stable phosphorylation of the 55 kDa protein (arrow) in calphoglin-expressing *E. coli*. Control, control vector-transfected *E. coli*; Native, native calphoglin-expressing *E. coli*; and Recombinant, C-terminal $(His)_6$-V5-tagged calphoglin-expressing *E. coli*. Ten microgram phosphorylated proteins were separated by SDS–PAGE on 12% gels, transferred onto PVDF, and autoradiography was performed. Chemical stability of phosphorylated proteins was determined by treating PVDF with 1 N HCl for 2 h. (B) Affinity-purified recombinant calphoglin protein compared to natural calphoglin in the cerebellum (CB). One microgram and 20 ng of bacterially expressed recombinant calphoglin on a filter are visualized in the left and central panels, respectively. Eighty kilodaltons of full-length calphoglin (filled triangle) and a secondary 35 kDa doublet of C-terminal calphoglin cleavage products (star) are shown. An immunoblot of 10 μg human cerebellum protein with anti-calphoglin antibodies demonstrates that calphoglin (open triangle) migrates with the size identical to that of bacterially expressed calphoglin. (C) Calphoglin-induced growth retardation of host *E. coli* cells. An empty pBluescript vector (control) and calphoglin cDNA in the vector were induced into BL21 cells where basal expression is leaky. (D) Calphoglin-induced PGM activation in *E. coli* cells. CALP, calphoglin. The activity was measured by determining the rate of glucose-6-phosphate formation. Five micrograms of cell extracts was used in the assay. Data are means ± SEM from three independent experiments. (E) The increased amount of cellular Pi in calphoglin-expressing *E. coli* cells. The increase in Pi level was calculated to be 1.7-fold. Data are means ± SEM from two independent experiments.

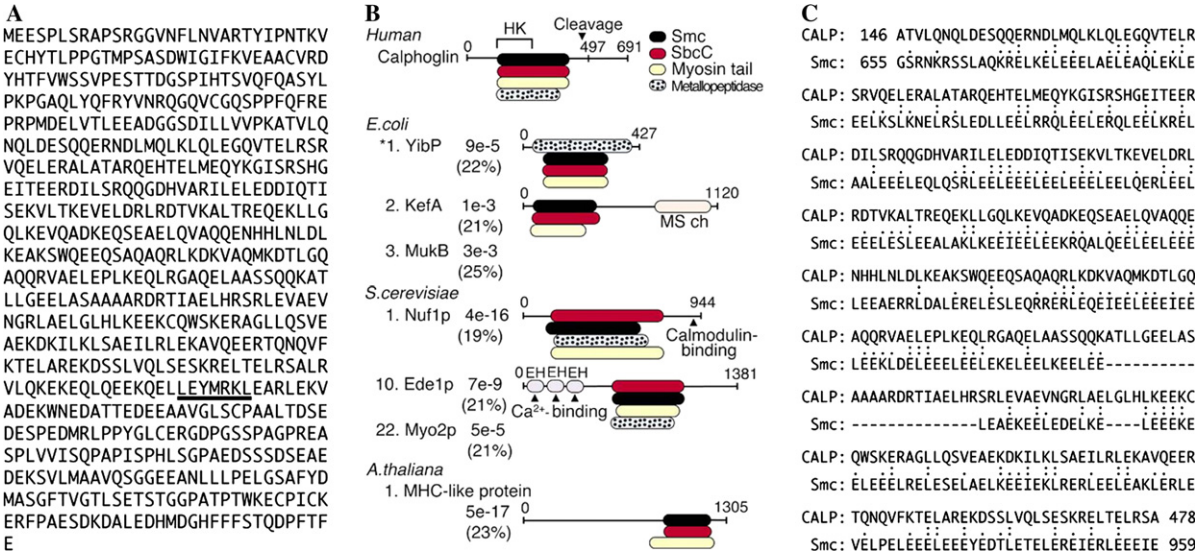

summation of a higher phosphorylation level and an accelerated substrate turnover. Of the other surveyed cellular parameters, the total cellular inorganic phosphate (Pi) level of calphoglin-expressing *E. coli* cells was significantly higher than the control (Fig. 1E, 1.7-fold).

Calphoglin has an evolutionarily conserved domain and is widely expressed in brain and other organs with ubiquitous co-localization with PGM

Calphoglin was initially a protein of unknown functions, but had a unique structure that differed from the "kinase" protein family. It showed low homology to a bacterial histidine kinase domain with an expect value of 0.036 and a percent identity of 24% (Fig. 2B, HK region), which was insufficient to predict protein function. However, a protein domain database search revealed the presence of a conserved domain in calphoglin, which is also found in Smc, Sbc, myosin tail, and metallopeptidase (Fig. 2B). Human calphoglin showed high homology to Smc, a chromosome segregation ATPase, with an expect value of 1e−13 and a percent identity of 26% (Fig. 2C). Moreover, the comparison of the top calphoglin homologues between *E. coli* and other eukaryotes showed a high degree (9e−5, 4e−16, and 5e−17, Fig. 2B) of conservation throughout evolution. Furthermore, these homologues had the conserved domain of Smc, Sbc, myosin tail, and metallopeptidase.

The cellular distribution of calphoglin was determined in mammals. Calphoglin mRNA is present and co-localizes with PGM in all surveyed mouse organs (Fig. 3A). Substantial levels of calphoglin mRNA are evident throughout adult rat brain, with the highest concentrations of mRNA seen in the hippocampal neurons and cerebellar granule cells (Fig. 3B). Calphoglin protein is enriched in extracts of the human cerebellum and migrates as a single 80 kDa band (Fig. 1B). The broad distribution of the calphoglin homologue, the equally balanced divergence, and the ubiquitous co-localization with PGM underlie the calphoglin-induced activation of *E. coli* PGM.

Co-localization of yeast PGM and calphoglin homologues within calmodulin protein complexes

Analysis of native yeast protein complexes by sensitive mass spectrometric methods allows the detection of "orthologue proteomes," which are thought to have evolved by vertical descent from a common ancestor and are presumed to carry out some of the core functions of cells [5]. Since PGM is universally conserved and its orthologues are found in all species, we searched the proteome-wide database of yeast protein complexes [5,6] using PGM as a probe to explore the intracellular pathway of calphoglin-induced PGM activation. An initial search identified 15 protein complexes that contain PGM. We found that one of them was enriched with

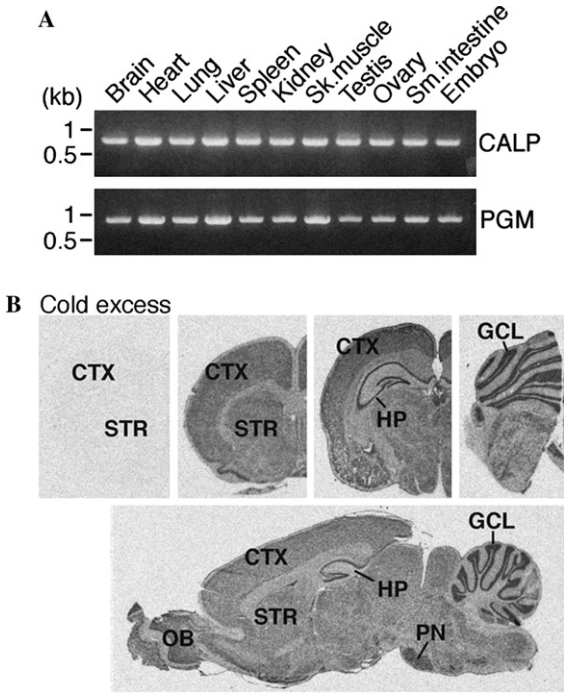

Fig. 3. Calphoglin is widely expressed in mammalian organs and brain cells with ubiquitous co-localization with PGM. (A) RT-PCR analysis of multiple mouse mRNA for calphoglin and PGM. Five nanograms of each organ cDNA was used as a template. After amplification cycles, reaction mixtures were electrophoresed on 1.2% agarose gels. The predicted sizes of PCR products with two specific primers for calphoglin and PGM are 738 and 886 bp, respectively. (B) In situ hybridization of calphoglin in rat brain coronal and sagittal sections. OB, olfactory bulb; CTX, cortex; STR, striatum; HP, hippocampus; PN, pontine nucleus; and GCL, granule cell layer. In order to verify the specificity of staining, adult striatum tissue sections were probed with ^{35}S-labeled calphoglin cRNA in the presence or absence of a 100-fold excess of unlabeled cRNA. The excess amount of cold probes abolished labeling, which indicates ubiquitous mRNA distribution in brain cells.

Fig. 2. Calphoglin has the unique structure with an evolutionarily conserved domain. (A) Amino acid sequence of calphoglin. An underline indicates N-terminal sequence of the 35 kDa fragment that was identified using a protein sequencer. A GenBank accession number for calphoglin cDNA is AY563137. (B) A schematic representation of the structural features of calphoglin and its homologues with homology data. *Numbers indicate high homology ranks in a homologue list of each species. The similarities are expressed as a combination of expect value and (percent identity). HK, region homologous to a histidine kinase; SbcC, ATPase involved in DNA repair; Smc, chromosomal segregation ATPase; MS ch, mechanosensitive channel; EH, Eps15 homology; and MHC, myosin heavy chain. (C) Aligned amino acid sequences of the homologous regions of human calphoglin and Smc. Identical amino acids between two sequences were labeled as ":", conservative substituted amino acids were labeled as ".". The numbers in the beginning and end of the alignment are the amino acid numbers starting with the first methionine. A NCBI Conserved Domain Number for Smc is COG1196.

calphoglin homologues while the remaining 14 complexes contained no homologues. This complex consists of 26 proteins (calmodulin protein as bait and 25 associated proteins) and includes at least three calphoglin homologues—Nuf1p, Ede1p, Myo2p, and other Myo proteins (Table 1 and Fig. 2B). Furthermore, the calmodulin complex is enriched with other highly conserved orthologues, and 10 of its components are essential proteins. The function of each component indicates the involvement of this complex in most elementary cell functions (RNA translation and basic metabolism) supporting the notion of an orthologue proteome. Some components such as calcineurin and cyclophilin mediate calcium signaling for neuronal activation and T cell proliferation. The 26 proteins are likely to be organized into some functional subunits around the mouth of intracellular Ca^{2+} channels. It is well known that Ede1p and Nuf1p, two calphoglin homologues present in the complex, are regulated by Ca^{2+} and calmodulin [19], respectively (Fig. 2B). KefA, an *E. coli* homologue for: calphoglin, Nuf1p, and Ede1p, forms a prokaryotic cation channel (Fig. 2B and Table 1) [20]. The homology of Nuf1p, Ede1p, and yeast PGM to their respective *E. coli* counterparts is high (3e−6, 2e−7, and 2e−17), and similar to that of other highly conserved orthologues within the calmodulin complex. These findings suggest the involvement of calphoglin in elementary cellular functions linked to Ca^{2+}/calmodulin signaling.

Functional assembly of calphoglin, IPP, and PGM proteins, and the conservation throughout evolution

The observation of the co-localization of yeast PGM and calphoglin homologues within the calmodulin protein complex has been followed up utilizing the yeast two-hybrid method [4] and other detailed functional studies. To explore whether calphoglin acts on PGM via a pathway within the calmodulin complex, yeast cDNAs of the calmodulin complex components were screened by two-hybrid methods using human calphoglin and *E. coli* PGM as baits (Fig. 4A). To provide direct evidence for the role of calphoglin in mediating universal cellular signals, we took advantage of the fact that calphoglin activates PGM in *E. coli* cells and used three different cDNA species (human calphoglin cDNA, *E. coli* PGM cDNA, and yeast cDNAs of complex components). As indicated by the arrows in Fig. 4A, yeast IPP was identified as a common interacting partner of human calphoglin and *E. coli* PGM, which indicates that the detected action of calphoglin on PGM may be bridged by an intermediary partner, *E. coli* IPP (Fig. 5A). Like PGM, IPPs are highly conserved enzymes that hydrolyze PPi to 2Pi and are present in all cellular organisms [21]. The functional assembly of a human calphoglin, a yeast IPP, and an *E. coli* PGM has proved the remarkable conservation of this pathway through billions of years of evolution. IPPs are required for a broad spectrum of PPi-releasing

Table 1
Yeast 26 proteins including calphoglin/calcineurin complexes and their mammalian and *E. coli* counterparts

Yeast protein	Mammalian orthologue	Homology[a] [Yeast to *E. coli*]	Top *E. coli* homologue	Function	Essential
Orthologue with evolutionarily conserved structure					
Vas1p	Valyl-tRNA synthetase	0 (43%)	Valyl-tRNA syn.	Translation, PPi release	Yes
Ils1p	Isoleucyl-tRNA synthetase	2e−84 (28%)	Isoleucyl-tRNA syn.	Translation, PPi release	Yes
Ynk1p	Nucleoside diphosphate kinase (NDK)	4e−30 (45%)	NDK	Nucleoside metabolism	No
Pgm2p	PGM	2e−17 (26%)	PGM	Glucose metabolism	No
Uba1p	Ubiquitin-activating enzyme	2e−15 (30%)	Thiamin biosyn. ThiF	Activation, PPi release	Yes
Calphoglin homologue					
Nuf1p	Calphoglin[b]	3e−6 (17%)	KefA and MukB	Part of spindle pole body	Yes
Ede1p	EH domain protein	2e−7 (20%)	KefA (second, YibP)	Endocytosis	No
Calcium signaling protein					
Cph1p	Cyclophilin	1e−8 (31%)	Peptidylprolyl isomerase	Calcineurin regulation	No
Cmp2p	Calcineurin	5e−3 (32%)	Protein phosphatase 2		No
Cmd1p	Calmodulin	0.43 (20%)	Not shown		Yes
Cmk2p	CaM kinase II	0.55 (25%)	ATP-binding protein		No
Myo2p	Class V MHC	0.09 (21%)	Pho regulon	Polarized growth	Yes
Myo3p,4p,5p	Class I, V, I, MHC	0.18–0.33 (30–27%)	Pho regulon		No, No, No
Other orthologue					
Ipp1p	IPP	4e−3 (31%)	IPP	PPi hydrolysis	Yes
Sod1p	Superoxide dismutase (SOD)	5e−6 (25%)	SOD		No
Hyp2p	Translation initiation factor eIF5A	0.83 (32%)	Isoleucyl-tRNA syn.	Translation	Yes
Other eight yeast proteins	(essential) Cof1p Mlc1p (non-essential) Hch1p Hul5p Pst2p She3p She4p Vps13p				

[a] Homology is expressed in expect value and (percent identity).
[b] Calphoglin is a mammalian homologue for Nuf1p.

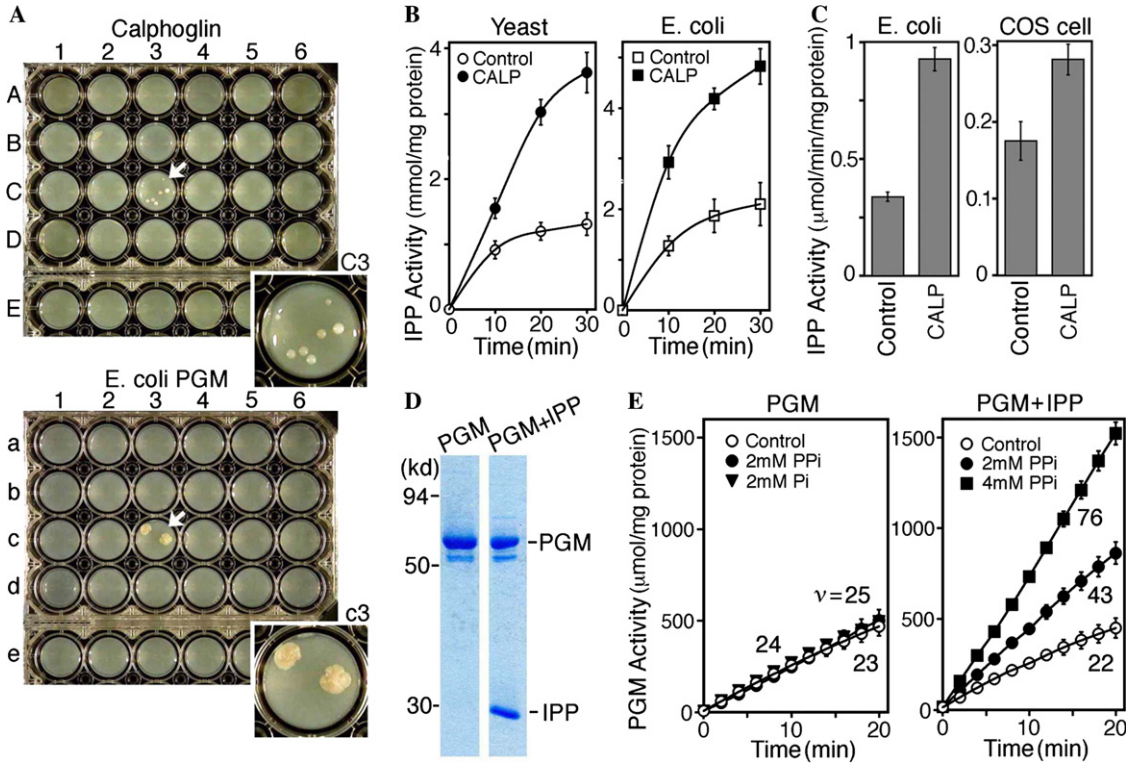

Fig. 4. Identification and functional analysis of the calphoglin complex. (A) Yeast two-hybid screening of a protein array of yeast calmodulin/calcineurin complex components. The DNA-binding domain vector pOBD2 and the Gal4 activation domain vector pOAD [12] were used. The screening was performed by transforming a plasmid of pOBD2-human *calphoglin* or pOBD2-*E. coli pgm* into a yeast reporter strain PJ69-4a expressing the following *S. cerevisiae* proteins as Gal4 activation domain fusions: Aa1, cmd1 (combination of well positions, protein name); Aa2, cmk2; Aa3, cmp2; Aa4, cph1; Aa5, cof1; Aa6, nuf1; Bb1, myo2; Bb2, myo3; Bb3, myo4; Bb4, myo5; Bb5, pgm2; Bb6, ils1; Cc1, vas1; Cc2, hyp2; Cc3, ipp1; Cc4, ynk1; Cc5, pst2; Cc6, sod1; Dd1, uba1; Dd2, vps13; Dd3, she4; Dd4, hch1; Dd5, hul5; Dd6, mlc1; Ee1, uso1; Ee2, myo1; Ee3, rad50; and Ee4, pgm1. In C3 and c3, colonies are shown (arrows) after three weeks of growth on medium lacking tryptophan, leucine, and histidine, and supplemented with 100 and 3 mM 3-amino-1,2,4-triazole, respectively, thus allowing growth only of cells that express the *his3* two-hybrid reporter gene. No colony was detected in other wells. (B) Calphoglin-dependent activity enhancement of the IPP proteins. Thirty nanograms of each purified IPP protein of yeast and *E. coli* (Sigma) was incubated with 300 ng of affinity-purified calphoglin protein for 10 min at 25 °C, and IPP activity was assayed for 30 min. The activity was measured by determining the amount of Pi liberated from PPi hydrolysis. Data are means ± SEM of three to four determinations from four independent experiments. (C) The increased IPP activities in 30 μg and 36 μg cell lysates of calphoglin-expressing *E. coli* and COS cells, respectively. Data are means ± SEM from three independent experiments. (D) CBB staining of 3 μg of affinity-purified proteins from single and double transformants. Host *E. coli* cells were singly transformed with the plasmid encoding $(His)_6$-tagged *E. coli* PGM, or doubly transformed with $(His)_6$-PGM plasmid and $(His)_6$-*E. coli* IPP plasmid. Double transformants were selected on plates containing ampicillin and chloramphenicol. (E) The functional characterization of the singly purified PGM is compared to that of the co-purified PGM with IPP protein. 0.15 μg of each PGM was used in the assay. Data are means ± SEM from four independent experiments.

biosynthetic pathways, including oligosaccharide and fatty acid synthesis, tRNA charging/amino acid activation (Table 1), and polynucleotide synthesis [22]. These biosyntheses are not thermodynamically favorable and are reversible reactions. The hydrolysis of PPi by IPP eliminates metabolite inhibition, therefore shifting the reaction equilibrium in favor of polymerization (Fig. 5A) [22].

To confirm the yeast two-hybrid results, we reconstituted calphoglin protein with yeast IPP and *E. coli* IPP in vitro, and monitored the functional interactions of the two proteins by enzyme activity assays (Fig. 4B). A purified recombinant calphoglin protein, not a control extract, was able to enhance the activity of the yeast IPP protein in vitro to 2.8-fold of the base level at 30 min. Similarly, calphoglin enhanced the protein activity of *E. coli* IPP. These results indicate that calphoglin directly interacts with and increases the activities of prokaryotic and eukaryotic IPPs. To further establish that calphoglin activates IPPs, IPP activity was determined in lysates of the calphoglin cDNA-transfected cell cultures of *E. coli* cells and mammalian COS cells (Fig. 4C). Consistent with the results of in vitro reconstitution, cellular expression of calphoglin enhanced *E. coli*'s and mammalian IPP activities by 2.5-fold and 1.6-fold of their base levels, respectively. The result explains that our initial finding of increased cellular Pi concentration (Fig. 1E) is due to calphoglin-induced IPP activation. Calphoglin defines the novel protein function of an IPP activator.

To investigate the IPP–PGM interaction, we co-expressed these recombinant proteins in *E. coli* in combi-

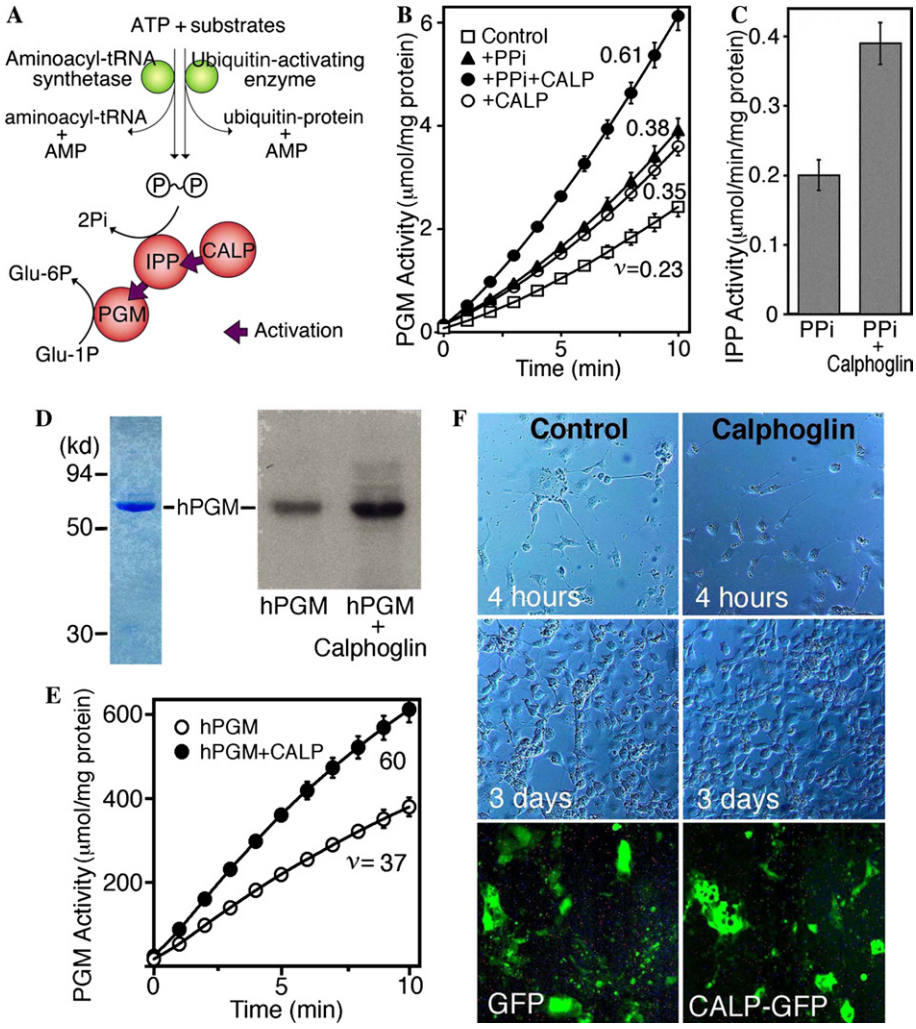

Fig. 5. Model and activity of the native calphoglin complex. (A) Proposed model of assembly and action of the calphoglin complex. (B,C) Activities of a native calphoglin complex in the soluble protein fraction of rat skeletal muscle. Twenty-five micrograms of a fraction protein was treated with: none (open squares), 2 mM PPi (filled triangles), 0.3 μg calphoglin (open circles), or 2 mM PPi and 0.3 μg calphoglin (filled circles), and PGM activities were assayed immediately. Similarly, IPP activities were determined with 85 μg muscle protein and 0.3 g calphoglin. Data are means ± SEM from three independent experiments. (D) Calphoglin-dependent enhancement of PGM autophosphorylation. Two micrograms of affinity-purified recombinant human PGM is visualized by CBB staining in the left panel. Ten micrograms of human calphoglin or control extract was incubated with 5 μg human PGM and 50 μM [^{32}P]ATP (50 μCi), and the phosphorylation of PGM was analyzed by autoradiography in the right panel. (E) Calphoglin-dependent enhancement of PGM enzymatic activity. 0.39 μg of human calphoglin (filled circles) or control extract (open circles) was incubated with 0.23 μg human PGM for 10 min at 25 °C, and PGM activity was assayed for 10 min. Data are means ± SEM from three independent experiments. (F) Cell growth of calphoglin-expressing COS cells. COS-7 cells were transfected with a GFP-tagged calphoglin plasmid and a GFP plasmid (control) at culture day 0. Cell numbers and GFP fluorescence were recorded at 4 h, 1, 2, and 3 days following transfection. Phase-contrast microscopy (top four panels) and fluorescence microscopy at day 3 (bottom two panels) are shown. To evaluate the growth rate, the base amount of cellular protein at day 3 was determined to be 0.14 ± 0.02 mg/3.3 cm dish.

nation with IPP and PGM, or PGM alone. The expressed proteins were affinity-purified (Fig. 4D), and the PGM activities were measured in the presence and absence of PPi (Fig. 4E). When PGM was expressed alone, the activity of the purified PGM protein showed a product–time plot with a velocity of 23 ± 2.5 μmol/min/mg of protein and was unaffected by PPi. In contrast, co-expression of PGM with IPP resulted in different plots with the increasing velocities of 22 ± 2.6, 43 ± 3.0, and 76 ± 3.1 μmol/min/mg of protein, depending on the PPi concentration. These results indicate that IPP directly interacts with and enhances the activity of PGM in the presence of PPi. To evaluate whether the stimulation of PGM activity is due to the production of Pi from PPi, we added Pi to PGM alone; PGM activity was unaffected by Pi, which suggests that PGM activation occurs by the interaction with PPi, IPP, and free energy. This line of evidence infers the model in which calphoglin enhances IPP activity, which subsequently enhances PGM activity (Fig. 5A).

Activity of native calphoglin complexes

To define the calphoglin complex model, which is based on the cDNA expression system and reconstitution studies, our findings were integrated with a more physiological approach using mammalian native protein complexes. We treated soluble protein fractions of rat skeletal muscle with PPi alone, with calphoglin alone, or with PPi and calphoglin, and monitored the activities of both IPP and PGM (Figs. 5B and C). Consistent with the result of the in vitro reconstituted PGM + IPP model, enhancement of PGM activity from 0.23 ± 0.02 to 0.38 ± 0.02 μmol/min/mg of protein was observed after the addition of 2 mM PPi, presumably by the action of IPP and PPi hydrolysis detected in the fraction. Treatment of the fraction with 2 mM PPi and calphoglin further enhanced the activities of both IPP and PGM, which is consistent with the model. However, the addition of calphoglin alone also stimulated the PGM activity to 0.35 ± 0.02 μmol/min/mg of protein, which suggests that some portion of the activation of PGM occurred from the direct action of calphoglin. Thus, the calphoglin complex is a universal cell apparatus, and controls Pi and glucose metabolism from bacteria to mammals.

To investigate the direct action of calphoglin on PGM, a recombinant human PGM was purified (Fig. 5D, left panel) and reconstituted with the human calphoglin in vitro. PGM activation was monitored by PGM phosphorylation (Fig. 5D, right panel) and enzyme activity (Fig. 5E). Purified PGM alone showed autophosphorylation activity, which is consistent with the result of recent reports [23]. A purified calphoglin protein directly enhanced the PGM autophosphorylation activity and its enzymatic activity from 37 ± 2.2 to 60 ± 3.0 μmol/min/mg of protein, indicating a novel type activator of PGM.

The over-expression of calphoglin significantly suppressed *E. coli* cell growth (Fig. 1C). However, it is likely that this is simply due to the metabolic imbalance caused by the excess stimulation of PGM activity. To examine the effect of human calphoglin on mammalian cell growth, we transfected COS cells with a green fluorescent protein (GFP)-tagged calphoglin plasmid or a GFP plasmid (control) and monitored their growth rate (Fig. 5F). The expressed proteins of calphoglin-GFP and GFP began to appear at culture day 1, and reached a maximum level in more than 70% of the cultured cells at days 2 and 3. The calphoglin-expressing cells grew at $105 \pm 12\%$ of the base rate of the control cells, and both cell types became confluent at day 3. This result indicates that calphoglin does not suppress mammalian cell division.

Calphoglin complex is a key apparatus in linking principal neuronal metabolism with calcium and calcineurin signaling

In the brain, localization of the highest concentrations of calphoglin mRNA is closely related to that of Ca^{2+}-linked major neurotransmission proteins such as NMDA glutamate receptors [24] and nitric oxide synthases [25]. The co-localization of the calphoglin complex with Ca^{2+}/calmodulin signaling complexes and PPi-releasing reactions might reflect the intracellular link between locally concentrated Pi/PPi/sugar-metabolites, Ca^{2+} sequestration, and neuronal activation. A ^{45}Ca ligand-blotting experiment with the three purified components of the calphoglin complex demonstrated that Ca^{2+} does bind to 35 kDa C-terminal fragments of calphoglin, and IPPs of *E. coli* and yeast, but not to PGM (Fig. 6A). The Ca^{2+}-binding activity of calphoglin corresponds with the Ca^{2+}-linked characteristics of Nuf1p and Ede1p. In contrast to the potentiation effect of calphoglin on both prokaryotic and eukaryotic IPPs, Ca^{2+} is known to strongly inhibit their activity via the CaPPi complex, a strong competitive inhibitor for MgPPi [26]. To examine the relationship between calphoglin-induced IPP enhancement with its Ca^{2+}-dependent inhibition, we reconstituted calphoglin and each IPP of *E. coli*, yeast, and rat muscle in the presence of 3, 30, and 300 μM Ca^{2+} (Fig. 6C). Calphoglin enhanced in a similar manner all three IPP activities at all stages of inhibition, indicating that the type of interaction is distinct from the binding competition of Ca^{2+}. Moreover, treatment of recombinant calphoglin with [^{32}P]ATP and rat cerebellum homogenate selectively phosphorylated the 35 kDa C-terminal fragments of calphoglin (Fig. 6B), implying that the C-terminal portion of calphoglin regulates the total activity of the calphoglin–IPP complex in coordination with Ca^{2+}. The N-terminus of full-length calphoglin is likely to block the access of kinase protein to its C-terminal portion. In a recent analysis of an alternative splicing form of human calphoglin, we identified another C-terminal truncated form at the downstream of the 548th amino acid. This C-terminal truncated form sustained a significant level of its protein activity, which support a notion of the C-terminal portion as a regulatory domain.

Pi and glucose-6-phosphate, two products of calphoglin complex reactions, are known to significantly enhance the amount of Ca^{2+} sequestration in cellular microsomes [15]. If calphoglin–IPP functions as a Ca^{2+} sensor for the calphoglin complex, IPP–PGM may function as an effector to cooperate with Ca^{2+} signaling (Fig. 6F). To examine the role of the calphoglin complex in Ca^{2+} transport, we reconstituted rat microsomal vesicles with calphoglin, IPP, PPi, and $^{45}Ca^{2+}$ in vitro. Calphoglin significantly enhanced both the rate and quantity of microsomal $^{45}Ca^{2+}$ uptake (Fig. 6D), presumably due to increased Pi concentration (Fig. 6F). Recent studies have further demonstrated that PGM phosphorylation and activities play a pivotal role in Ca^{2+} flux in diverse species, consistent with our finding that calphoglin increased the ^{32}P-labeling level and activity of PGM. In studies using rat muscle sarcoplasmic reticulum [27] and some protozoa [28,29], PGM

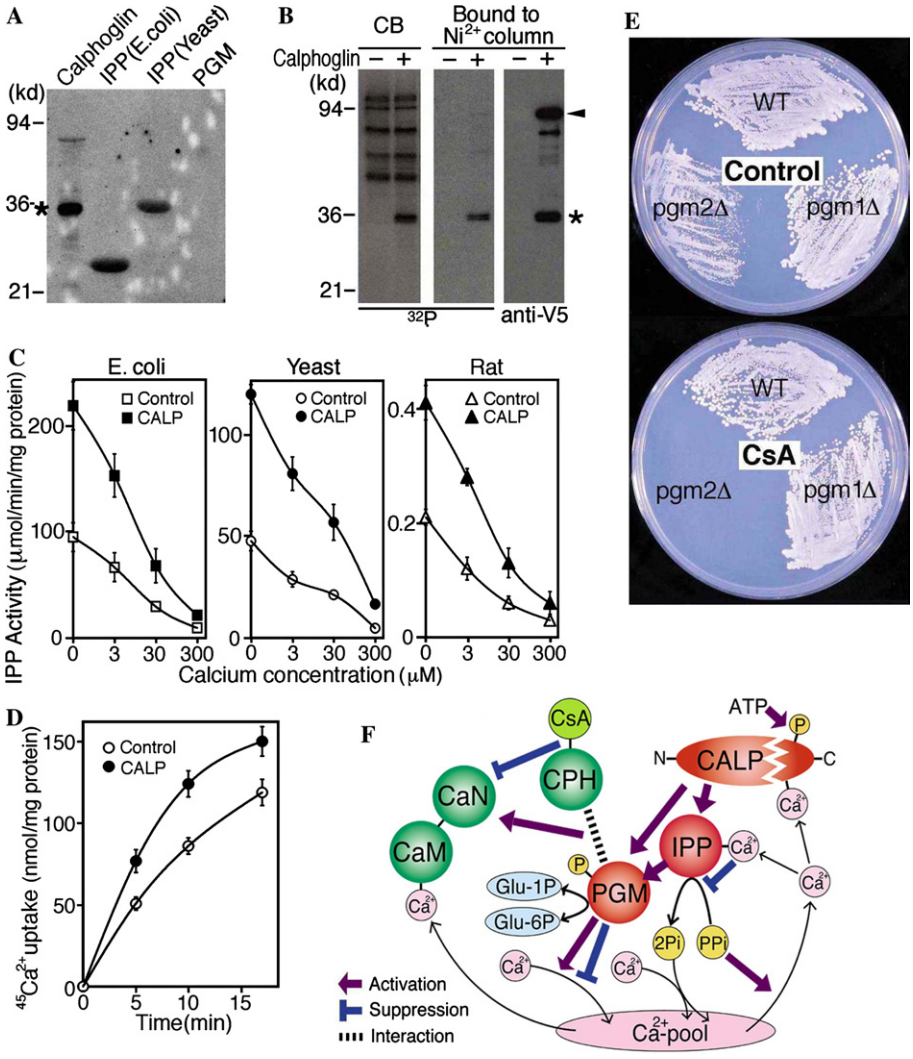

Fig. 6. Link of the calphoglin complex to calcium signaling. (A) Autoradiography of $^{45}Ca^{2+}$-bound calphoglin complex proteins on filter. About 1 μg of 35 kDa C-terminal calphoglin fragments (star) was separated by SDS–PAGE from 30 μg of total the recombinant protein extract. One microgram of each IPP and PGM from Sigma. (B) Cerebellar protein-dependent phosphorylation of 35 kDa C-terminal fragments of calphoglin. Thirty micrograms of recombinant calphoglin or control extract was incubated with 300 μg cerebellum homogenate and 300 μCi [^{32}P]ATP in a total volume of 250 μl, and the phosphorylation of the mixed proteins was analyzed by autoradiography (left). From 200 μl of the reactions, phosphorylated calphoglins were affinity-purified. The extracts were then analyzed by both autoradiography (center) and immunoblotting (right). An 80 kDa band of full-length calphoglin (filled triangle) and 35 kDa calphoglin fragments (star) are shown. (C) The effect of calphoglin on Ca^{2+}-dependent inhibition of IPPs of *E. coli*, yeast, and rat. Both purified IPPs of *E. coli* and yeast, and rat muscle proteins were used. Data are means ± SEM of three to four determinations from five independent experiments. (D) Calphoglin-induced enhancement of rat muscle microsomal $^{45}Ca^{2+}$ uptake in the reconstituted system. Data are means ± SEM from three independent experiments. (E) A potent inhibitor of calcineurin selectively inhibited cell growth of the pgm2Δ strain. The following strains (accession number) were obtained from EUROSCARF: wild type of BY4743 (Y20000), pgm1Δ (Y34977), and pgm2Δ (Y36545). The strains were plated on synthetic medium containing 2% galactose in the presence and absence of 10 μM CsA. The plates were incubated at 30 °C for 3 days. (F) Model of links between calcineurin/calphoglin complex and cellular calcium signaling. CPH, cyclophilin; CaN, calcineurin; and CaM, calmodulin.

and its paralogues were rapidly and extensively labeled with [^{32}P]ATP by a Ca^{2+}/calmodulin-dependent mechanism, correlated to the Ca^{2+} release factor.

Further, we performed a yeast proteome database search using each component of the 26 yeast proteins and identified a key pathway to link the function of calphoglin to calcium/calcineurin signaling. We found that four of the 15 PGM-containing complexes contained cyclophilin (Cph1p, an endogenous inhibitor for calcineurin). Yeast has two PGM isoforms, Pgm1p and Pgm2p, but all four complexes contained Pgm2p, one of the 26 components of the calmodulin protein complex (Table 1). This intensive intracellular co-localization indicates that Pgm2p directly binds to cyclophilin (Fig. 6F) because they were co-purified by four different bait proteins. Like calphoglin, cyclophilin is an evolutionarily conserved component of eukaryotic calcium signaling (1e−8, Table 1).

A recent report supports the results from our yeast proteome database search. It was shown that a yeast

mutant lacking Pgm2p (pgm2Δ) accumulates a 9-fold higher level of steady-state total cellular Ca^{2+} and that its growth was inhibited by CsA, a potent inhibitor of calcineurin [30]. To determine the specific link between Pgm2p and calcium/calcineurin signaling, we performed experiments using yeast PGM deletion mutant strains (Fig. 6E). The effects of 10 μM CsA on growth of wild type, pgm1Δ (another PGM isoform that is not included in the 26 protein complex), and pgm2Δ strains were examined. We found that growth of the wild type and pgm1Δ strains was unaffected by CsA, while growth of the pgm2Δ strains was completely suppressed. This line of evidence demonstrates the essential roles of pgm2p and calcineurin in cellular Ca^{2+} signaling, and that the activities of both proteins regulate cell growth in coordination with each other in the calmodulin complex. Thus, the Pgm2p–cyclophilin interactions in the 26 proteins provide a molecular basis for how PGM influences calcineurin signaling and cellular proliferation (Fig. 6F).

Acknowledgments

We thank Stanley Fields for all of the yeast clones used in the two-hybrid assay, and Katsuei Shibuki for his generous support. We also like to thank Saeko Maruyama and Shouichi Oyanagi for their technical assistance.

References

[1] S. Vaulont, M. Vasseur-Cognet, A. Kahn, Glucose regulation of gene transcription, J. Biol. Chem. 275 (2000) 31555–31558.
[2] S.L. Schreiber, G.R. Crabtree, The mechanism of action of cyclosporin A and FK506, Immunol. Today 13 (1992) 136–142.
[3] S.H. Snyder, D.M. Sabatini, M.M. Lai, J.P. Steiner, G.S. Hamilton, P.D. Suzdak, Neural actions of immunophilin ligands, Trends Pharmacol. Sci. 19 (1998) 21–26.
[4] P. Uetz, L. Giot, G. Cagney, T.A. Mansfield, R.S. Judson, J.R. Knight, D. Lockshon, V. Narayan, M. Srinivasan, P. Pochart, A. Qureshi-Emili, Y. Li, B. Godwin, D. Conover, T. Kalbfleisch, G. Vijayadamodar, M. Yang, M. Johnston, S. Fields, J.M. Rothberg, A comprehensive analysis of protein–protein interactions in *Saccharomyces cerevisiae*, Nature 403 (2000) 623–627.
[5] A.C. Gavin, M. Bosche, R. Krause, P. Grandi, M. Marzioch, A. Bauer, J. Schultz, J.M. Rick, A.M. Michon, C.M. Cruciat, M. Remor, C. Hofert, M. Schelder, M. Brajenovic, H. Ruffner, A. Merino, K. Klein, M. Hudak, D. Dickson, T. Rudi, V. Gnau, A. Bauch, S. Bastuck, B. Huhse, C. Leutwein, M.A. Heurtier, R.R. Copley, A. Edelmann, E. Querfurth, V. Rybin, G. Drewes, M. Raida, T. Bouwmeester, P. Bork, B. Seraphin, B. Kuster, G. Neubauer, G. Superti-Furga, Functional organization of the yeast proteome by systematic analysis of protein complexes, Nature 415 (2002) 141–147.
[6] Y. Ho, A. Gruhler, A. Heilbut, G.D. Bader, L. Moore, S.L. Adams, A. Millar, P. Taylor, K. Bennett, K. Boutilier, L. Yang, C. Wolting, I. Donaldson, S. Schandorff, J. Shewnarane, M. Vo, J. Taggart, M. Goudreault, B. Muskat, C. Alfarano, D. Dewar, Z. Lin, K. Michalickova, A.R. Willems, H. Sassi, P.A. Nielsen, K.J. Rasmussen, J.R. Andersen, L.E. Johansen, L.H. Hansen, B.D. Jespersen, A. Podtelejnikov, E. Nielsen, J. Crawford, V. Poulsen, B.D. Sorensen, J. Matthiesen, R.C. Hendrickson, F. Gleeson, T. Pawson, M.F. Moran, D. Durocher, M. Mann, C.W. Hogue, D. Figeys, M. Tyers, Systematic identification of protein complexes in *Saccharomyces cerevisiae* by mass spectrometry, Nature 415 (2002) 180–183.
[7] P.M. Wolanin, P.A. Thomason, J.B. Stock, Histidine protein kinases: key signal transducers outside the animal kingdom, Genome Biol. 3 (2002) REVIEWS3013.
[8] M. Lasker, C.D. Bui, P.G. Besant, K. Sugawara, P. Thai, G. Medzihradszky, C.W. Turck, Protein histidine phosphorylation: increased stability of thiophosphohistidine, Protein Sci. 8 (1999) 2177–2185.
[9] P.J. Kennelly, Archaeal protein kinases and protein phosphatases: insights from genomics and biochemistry, Biochem. J. 370 (2003) 373–389.
[10] J.K. Heinonen, R.J. Lahti, A new and convenient colorimetric determination of inorganic orthophosphate and its application to the assay of inorganic pyrophosphatase, Anal. Biochem. 113 (1981) 313–317.
[11] T. Ingi, Y. Aoki, Expression of RGS2, RGS4 and RGS7 in the developing postnatal brain, Eur. J. Neurosci. 15 (2002) 929–936.
[12] G. Cagney, P. Uetz, S. Fields, High-throughput screening for protein–protein interactions using two-hybrid assay, Methods Enzymol. 328 (2000) 3–14.
[13] K. Maruyama, T. Mikawa, S. Ebashi, Detection of calcium binding proteins by ^{45}Ca autoradiography on nitrocellulose membrane after sodium dodecyl sulfate gel electrophoresis, J. Biochem. (Tokyo) 95 (1984) 511–519.
[14] S. Eletr, G. Inesi, Phospholipid orientation in sarcoplasmic membranes: spin-label ESR and proton MNR studies, Biochim. Biophys. Acta 282 (1972) 174–179.
[15] R. Fulceri, G. Bellomo, A. Gamberucci, A. Romani, A. Benedetti, Physiological concentrations of inorganic phosphate affect MgATP-dependent Ca^{2+} storage and inositol trisphosphate-induced Ca^{2+} efflux in microsomal vesicles from non-hepatic cells, Biochem. J. 289 (1993) 299–306.
[16] M. Lu, N. Kleckner, Molecular cloning and characterization of the pgm gene encoding phosphoglucomutase of *Escherichia coli*, J. Bacteriol. 176 (1994) 5847–5851.
[17] B. Solow, K.M. Bischoff, M.J. Zylka, P.J. Kennelly, Archael phosphoproteins. Identification of a hexosephosphate mutase and the α-subunit of succinyl-CoA synthetase in the extreme acidothermophile *Sulfolobus solfataricus*, Protein Sci. 7 (1998) 105–111.
[18] G.I. Rhyu, W.J. Ray Jr., J.L. Markley, Enzyme-bound intermediates in the conversion of glucose 1-phosphate to glucose 6-phosphate by phosphoglucomutase. Phosphorus NMR studies, Biochemistry 23 (1984) 252–260.
[19] M.S. Cyert, Genetic analysis of calmodulin and its targets in *Saccharomyces cerevisiae*, Annu. Rev. Genet. 35 (2001) 647–672.
[20] D. McLaggan, M.A. Jones, G. Gouesbet, N. Levina, S. Lindey, W. Epstein, I.R. Booth, Analysis of the kefA2 mutation suggests that KefA is a cation-specific channel involved in osmotic adaptation in *Escherichia coli*, Mol. Microbiol. 43 (2002) 521–536.
[21] B.S. Cooperman, A.A. Baykov, R. Lahti, Evolutionary conservation of the active site of soluble inorganic pyrophosphatase, Trends Biochem. Sci. 17 (1992) 262–266.
[22] A. Kornberg, On the Metabolic Significance of Phosphorolytic and Pyrophosphorolytic Reactions, Academic Press, New York, 1962.
[23] L. Jolly, F. Pompeo, J. van Heijenoort, F. Fassy, D. Mengin-Lecreulx, Autophosphorylation of phosphoglucosamine mutase from *Escherichia coli*, J. Bacteriol. 182 (2000) 1280–1285.
[24] K. Moriyoshi, M. Masu, T. Ishii, R. Shigemoto, N. Mizuno, S. Nakanishi, Molecular cloning and characterization of the rat NMDA receptor, Nature 354 (1991) 31–37.

[25] D.S. Bredt, P.M. Hwang, C.E. Glatt, C. Lowenstein, R.R. Reed, S.H. Snyder, Cloned and expressed nitric oxide synthase structurally resembles cytochrome P-450 reductase, Nature 351 (1991) 714–718.

[26] S.M. Avaeva, N.N. Vorobyeva, S.A. Kurilova, T.I. Nazarova, K.M. Polyakov, E.V. Rodina, V.R. Samygina, Mechanism of Ca^{2+}-induced inhibition of *Escherichia coli* inorganic pyrophosphatase, Biochemistry (Mosc.) 65 (2000) 373–387.

[27] Y.S. Lee, A.R. Marks, N. Gureckas, R. Lacro, B. Nadal-Ginard, D.H. Kim, Purification, characterization, and molecular cloning of a 60-kDa phosphoprotein in rabbit skeletal sarcoplasmic reticulum which is an isoform of phosphoglucomutase, J. Biol. Chem. 267 (1992) 21080–21088.

[28] S.V. Subramanian, E. Wyroba, A.P. Andersen, B.H. Satir, Cloning and sequencing of parafusin a calcium-dependent exocytosis-related phosphoglycoprotein, Proc. Natl. Acad Sci. USA 91 (1994) 9832–9836.

[29] K. Hauser, R. Kissmehl, J. Linder, J.E. Schultz, F. Lottspeich, H. Plattner, Identification of isoforms of the exocytosis-sensitive phosphoprotein PP63/parafusin in *Paramecium tetraurelia* and demonstration of phosphoglucomutase activity, Biochem. J. 323 (1997) 289–296.

[30] L. Fu, A. Miseta, D. Hunton, R.B. Marchase, D.M. Bedwell, Loss of the major isoform of phosphoglucomutase results in altered calcium homeostasis in *Saccharomyces cerevisiae*, J. Biol. Chem. 275 (2000) 5431–5440.